Research Article

Meriem F. Bouali, Mahdi O. Karkush*, and Mounir Bouassida

Impact of wall movements on the location of passive Earth thrust

https://doi.org/10.1515/geo-2020-0248
received December 14, 2020; accepted April 08, 2021

Abstract: The general assumption of linear variation of earth pressures with depth on retaining structures is still controversial; investigations are yet required to determine those distributions of the passive earth pressure (PEP) accurately and deduce the corresponding centroid location. In particular, for rigid retaining walls, the calculation of PEP is strongly dependent on the type of wall movement. This paper presents a numerical analysis for studying the influence of wall movement on the PEP distribution on a rigid retaining wall and the passive earth thrust location. The numerical predictions are remarkably similar to existing experimental works as recorded on scaled test models and full-scale retaining walls. It is observed that the PEP varies linearly with depth for the horizontal translation, but it is nonlinear when the movement is rotational about the top of the retaining wall. When rotation is around the top of the wall, the resultant of PEP is located at a depth that varies between 0.164 and 0.259H of the wall height measured from the base of the wall, which is lesser than 1/3 of the wall height. The passive earth thrust location is highly affected by the soil–wall friction angle, especially when the friction angle of the backfill material increases. Despite the herein presented results, further experiments are recommended to assess the corresponding numerical predictions.

Keywords: passive pressure, numerical analysis, rotation, translation movement, wall

*** Corresponding author: Mahdi O. Karkush,** Department of Civil Engineering, University of Baghdad, Baghdad, Iraq,
e-mail: mahdi_karkush@coeng.uobaghdad.edu.iq
Meriem F. Bouali: Department of Civil Engineering, University of Mohamed Chérif Messaadia, Souk Ahras, Algeria,
e-mail: m.bouali@univ-soukahras.dz
Mounir Bouassida: Department of Civil Engineering, Ecole Nationale d'Ingénieurs de Tunis, Université de Tunis El Manar, Tunis, Tunisia,
e-mail: mounir.bouassida@enit.utm.tn

1 Introduction

Earth pressure distribution is an important condition for the economical and secure design of retaining walls, sheet piles, and diaphragm walls. The soil pressures determined by the theory of Rankine [1] or Coulomb [2] assumed a linear surface of failure and the resultant of the passive earth pressure (PEP) is located at 1/3H measured from the wall base. The geotechnical engineers still follow these ideas in the analysis and design of retaining walls until now. Several experimental studies suggested that the movement of the wall greatly affects the distribution of PEP and its centroid [3–9]. Based on the existing contributions in this field, the coefficient of PEP (K_p) and the normalized depth (h/H) where the resultant of PEP acts are considered the key parameters in estimating the distribution of PEP. Literature review showed that few investigations are available as related to PEP induced by retaining walls. Earlier, Fang et al. (1994) [4] studied different displacement modes and various densities of sand to analyze the distribution of PEP.

Later, Fang et al. (2002) [10] conducted series of experiments dealing with PEP distribution using loose cohesionless backfill material. Those authors concluded that the passive pressure distribution is linear and in good agreement with a classical solution.

Recently, Dou et al. [5] carried out experimental and analytical investigations for studying the distribution of the passive soil pressure exerted on a wall model subjected to rotation around its top. Those authors analyzed the effect of relative density of the backfill material on PEP distribution and the centroid of passive earth force.

Regarding analytical contributions, the solution provided by Kérisel and Absi [11] enables the effect of soil–wall frictional contact to derive the PEP.

Studying the effects of the types of movement on the distribution of PEP exerted on a retaining wall is very useful because of its substantial importance in the practice of design and analysis of retaining structures. As the first example, coal mining activities and ships operations during berthing represent some of the main applications

of induced passive earth stress by quay wall. The second example corresponds to buildings comprising basement levels when subjected to the wind solicitation and also generates the passive earth state.

The numerical analysis applications have been extended to several problems; it has been concluded that such tools are suitable to analyze geotechnical problems [12–16]. However, the FEM requires calibration by selecting appropriate parameters or a soil constitutive model. Accordingly, this numerical investigation's main objective is to investigate the distribution of PEP on a rigid retaining wall subjected to a horizontal translation movement and rotational movement around its top. Applicability of the translation and rotation movements is essentially viewed from the in situ observed failure modes. Meanwhile, one can adopt that translation movement applies for soil failure only produced over the retaining structure's height. However, rotation failure mode essentially involves in a more significant volume of landslide surrounding the retaining structure. In this paper, a numerical analysis is performed to predict a purely frictional soil behavior subject to translation and rotation movements by a rigid wall. The computed passive earth force, for different values of the interface soil–wall resistance, is compared to existing analytical and experimental results. Two main parameters govern the passive earth force: its intensity and normalized location with respect to normalized location regarding the rigid wall height. Therefore, the present work focuses on the determination of PEP induced by two types of rigid wall movements, e.g., translation and rotation around the top, on which very few contributions exist. Indeed, the proposed results highlighted the significant influence of the type of wall movement on the distribution and the resultant of PEP for cohesionless backfill material.

2 Numerical analysis

A numerical model is adopted to predict the PEP distribution on a rigid wall undergoing two movement types. The first type of movement is a horizontal translation (T), where S represents the maximum uniform horizontal displacement as shown in Figure 1a. The second type of movement is a rotation around the top of the wall (RT) (Figure 1b), where θ indicates the rotation angle. In both cases, the PEP is mobilized along with a purely frictional contact between the soil and the wall.

A rigid retaining wall model is analyzed in plane strain condition using 2D finite-difference element code FLAC [17]. The cohesionless backfill material is assumed

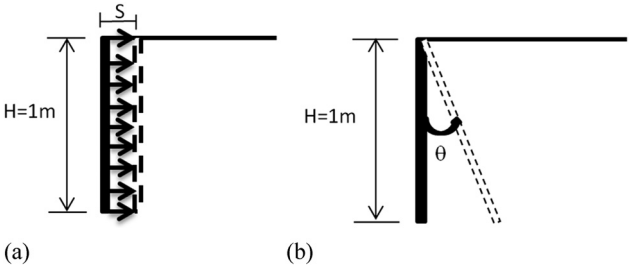

Figure 1: Assumed wall movements. (a) Translation, (b) rotation about top.

dry and homogenous. Preliminary numerical trials were implemented to select the suitable geometry of retaining wall, size of mesh, boundary conditions, and rate of displacements, (S in T movement) and (θ in RT movement), applied at the nodes over the wall height. Figure 2 shows the geometry of the wall model of 1 m height. Following the guidelines provided in FLAC [17], the dimensions of the soil model are chosen to be equal to 6 times the wall height in horizontal (x coordinate) and vertical (y coordinate) directions to mitigate the boundary effects. Boundary conditions are the following (Figure 2):

- At $x = 6H$ and $0 \le y \le 6H$, only vertical displacement is permitted.
- Two different boundary conditions are adopted at $x = 0$ and $0 \le y \le 6H$:
  (1) $x = 0$ and $5H \le y \le 6H$, there are two cases: uniform horizontal displacement as shown in Figure 1a and rotational displacement as shown in Figure 1b.
  (2) $x = 0$ and $0 \le y < 5H$, the horizontal displacement is zero; the vertical displacement is allowed.
- $y = 0$ and $0 \le x \le 6H$, the horizontal and vertical displacements are not allowed (zero values).

Several numerical models were performed to choose the most appropriate one to ensure that the developed failure surface is entirely located in the backfill material, i.e., it does not intercept the vertical right-hand boundary. The mesh size is refined near the wall-soil interface, where the maximum deformations are distributed, as shown in Figure 2. The discretization of the experimental model requires introducing a suitable interface element to characterize the friction soil–wall contact. Hence, joints of zero thickness are used to simulate the interface element. The cohesionless interface is characterized by a normal stiffness $K_n = 10^3$ MPa/m and a shear stiffness $K_s = 10^3$ MPa/m; the frictional contact at the soil and wall interface takes the following normalized values: $\delta/\varphi = 0$; 1/3; 1/2; 2/3; 1. The friction angle of the backfill material (φ) varies as 20, 25, 30, 35, and 40° (Fang et al. 1994) [4]. Following the recommendations given in the FLAC [17] users guide, the values of

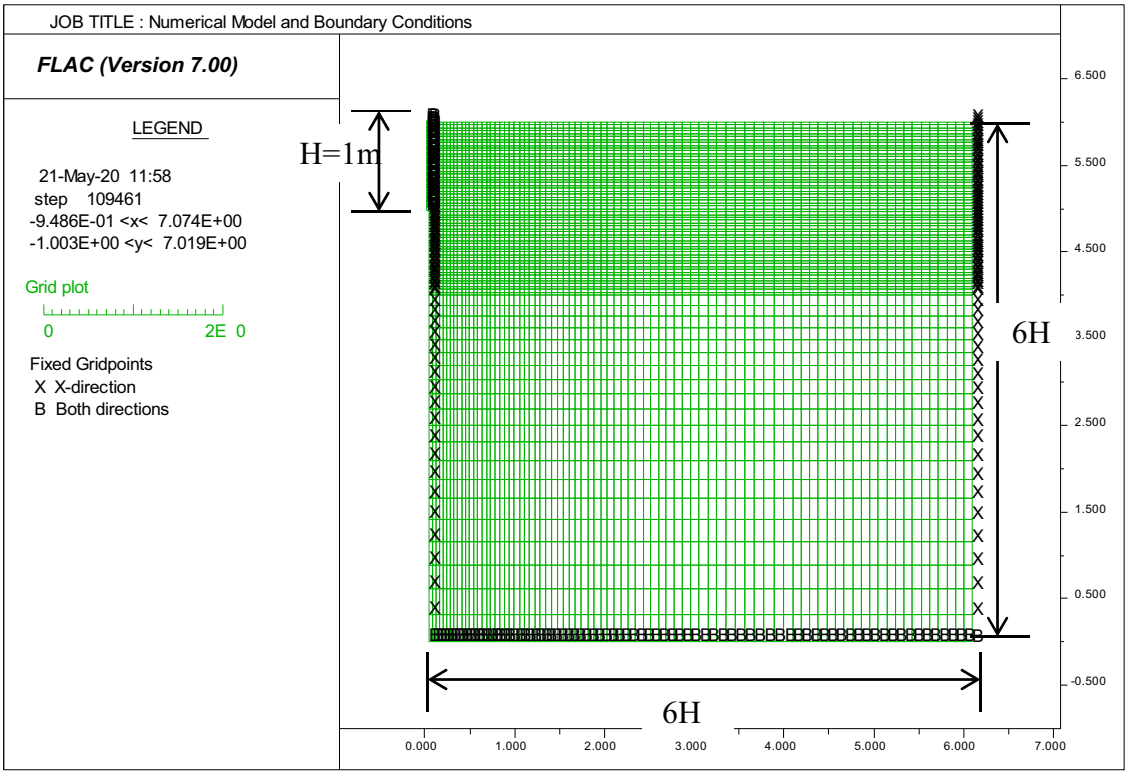

Figure 2: The adopted mesh of the proposed numerical model.

normal and tangent stiffnesses, K_n and K_s, of the soil–wall interface are assumed equal ten times the equivalent stiffness of the adjacent element. The stress–strain behavior of soil is supposed to be linear elastic-perfectly plastic and to obey Mohr–Coulomb failure criteria with related flow rule. The soil properties are: unit weight (γ) is 20 kN/m^3, the Young modulus (E) is 27 MPa, Poisson's ratio (ν) is 0.35, the shear modulus (G) is 10 MPa, and the bulk modulus (K) is 30 MPa [18]. It is noted that the magnitude of the PEP coefficient (K_p) does not depend on the soil's elastic properties [19].

The rigid retaining wall moves towards the backfill material to create the passive soil failure. In the case of the translation movement (T), a prolonged displacement rate of 10^{-6} m/step is applied to all wall elements (Figure 3a). For the rotational movement (RT), a rotation angle of magnitude 2.10^{-4} rad is applied around the wall's top edge (Figure 3b). As the wall starts to move towards the soil, a steady plastic flow is induced in it, which is accompanied by gradual increase in the PEP. The corresponding PEP to the displacement causing the plastic condition describes the ultimate passive earth force as shown in Figure 4, where P_p corresponds to the ultimate passive force's recorded asymptotic value. Hence, the coefficient of PEP (K_p) can be calculated using equation (1):

$$K_p = 2P_p/(\gamma H^2 \cos \delta) \quad (1)$$

The centroid of the resultant of the PEP is normalized to the wall height (h/H); where h is the distance between the wall base and the location of the PEP resultant.

3 Results and discussion

3.1 Analysis of rigid wall under translation movement

Assessment of the numerical model's predictions is carried out through comparison with available experimental results and theoretical solutions of the PEP coefficient (K_p), the PEP distribution, and the centroid of the PEP force.

3.2 Predictions of the coefficient of PEP (K_p)

First, K_p's numerical results are compared with the existing solutions offered in research [11,18,20]. Figures 5 and 6 show the variation of PEP coefficient (K_p) obtained from

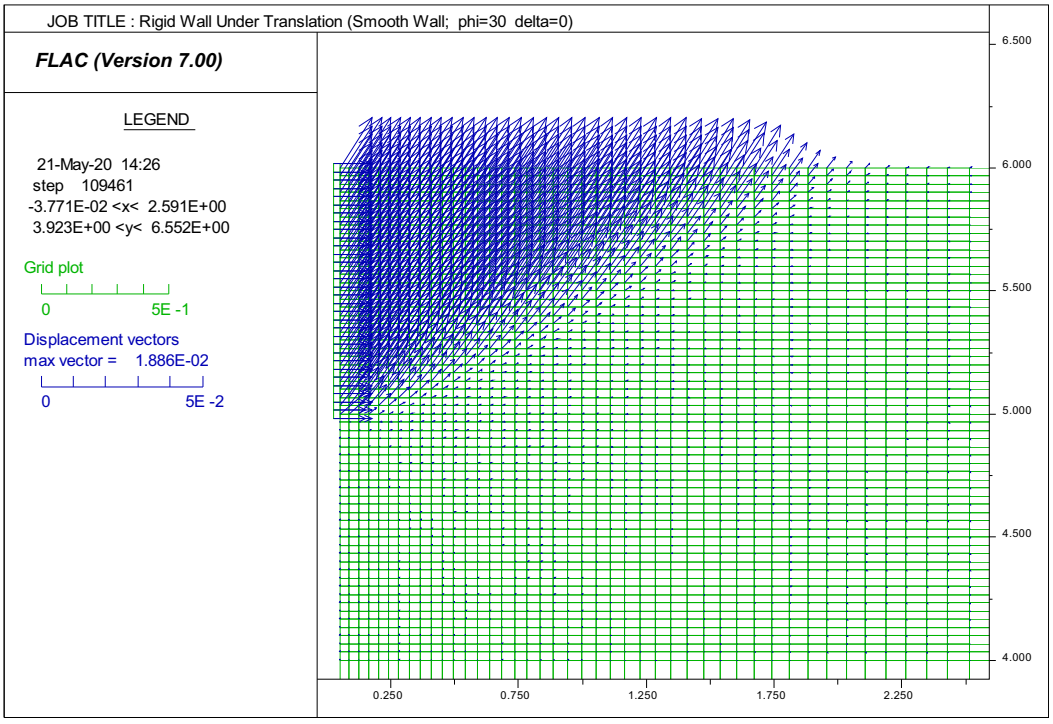

(a)

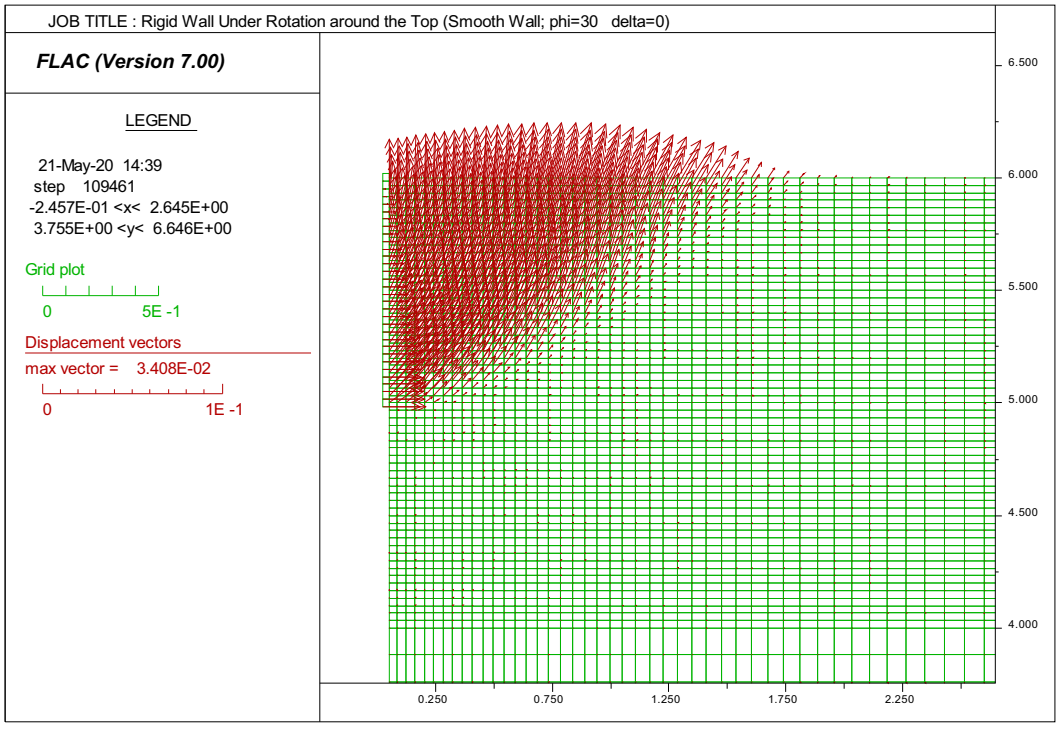

(b)

Figure 3: Predicted displacements field in the backfill material at the passive state. (a) Translation movement (*T*), (b) rotation around the top (RT).

those existing solutions versus the friction angle of backfill material (φ) and the angle of frictional contact between the soil and the wall (δ). Four prediction methods are considered, including the analytical methods suggested in ref. [11,20]. Numerical predictions correspond to the present analysis and the analysis by Benmeddour et al. [18].

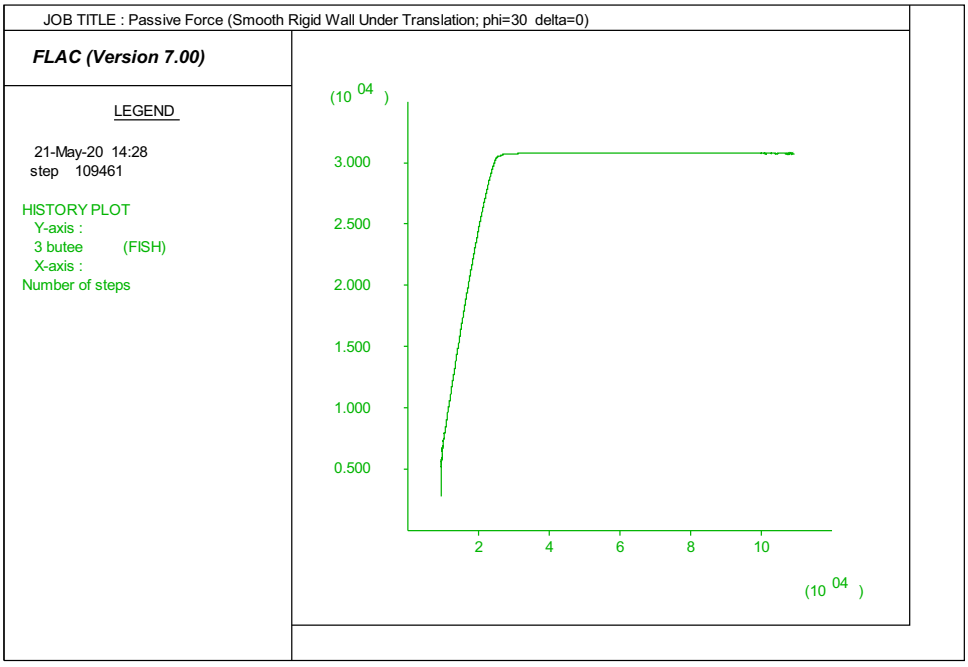

Figure 4: Variation of the passive earth force versus the number of iterations.

Note that Benmeddour et al. [18] did not calculate the K_p value for $\delta = \varphi$. Figure 6 shows the comparison corresponding to this case only considered with ref. [11,20].

From Figure 5, it is clear that in the range $0 \le \delta/\varphi \le 1/3$, the proposed numerical and analytical methods lead to the same value of the PEP coefficient K_p. A little difference between K_p values is noted when the backfill material's friction angle exceeds 35°. The conservative prediction is that obtained by the present analysis; the maximum prediction of K_p corresponds to the research proposed by ref. [20]. In turn, from $\delta/\varphi = 2/3$ to 1, Figure 6 shows significant differences between the values of K_p obtained by the present analysis and the existing numerical and analytical methods. For the most considered assumption, i.e., $\delta/\varphi = 2/3$, the maximum difference is marked between K_p values 6 and 7 for $\varphi = 35°$, then between 10.8 and 12.5 for $\varphi = 40°$. This difference becomes more remarkable when assuming a total adhesion between the soil and wall interface: $\delta = \varphi$. Regardless the relative differences between the results herein presented and those proposed by Kérisel and Absi [11] and Soubra and Macuh [20], one notes that the kinematic approach of limit analysis often provides an upper bound solution that is visible from Figure 6. Absi and Kérisel's analytical solution is found between the upper bound solution and the proposed numérical results deduced from FLAC 2D code. The latter, as perceived as an

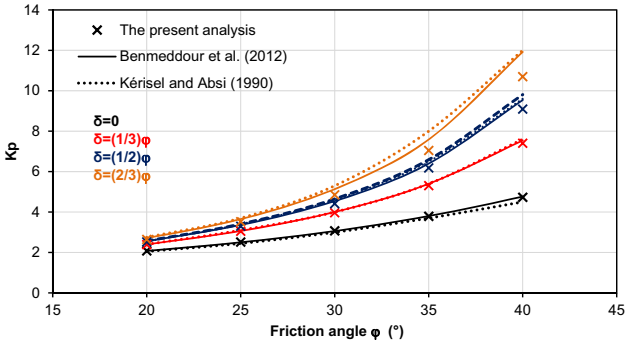

Figure 5: Analytical and numerical K_p values versus friction angle of backfill material for different interface friction angles (δ/φ = 0, 1/3, 1/2, 2/3).

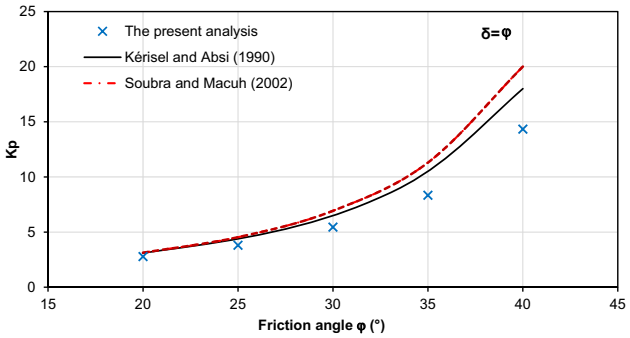

Figure 6: Variation of K_p with the friction angle (φ) of backfill material for $\delta = \varphi$.

approximation of an exact solution, may lead to underestimated predictions.

3.3 PEP distribution

Figure 7 shows the normalized distribution of PEP on a rigid vertical wall, where the earth pressure is divided by the overburden pressure (γH), and the depth (z) is divided by the wall height (H). Linear variation of the PEP is almost predicted over 90% of the rigid wall height; meanwhile, close to the wall base, a nonlinear variation of the PEP is obtained, particularly in case of a perfectly rough wall ($\delta = \varphi$). First, the results shown in Figure 7 indicate that the present numerical investigation's predictions are confirmed by the analytical solution proposed by the Rankine's theory up to a depth that equals $0.93H$. The nonlinearity observed at the wall base is attributed to the boundary conditions applied to the node in discretizing the wall by the finite-difference method. One notes that the increase in the angle of friction of the soil–wall contact causes the PEP growth with an exception made to the case $\delta = \varphi$.

Figure 8 shows the variation of maximum shear strains behind the rigid wall undergoing a translation movement in cases of the smooth soil–wall interface ($\delta = 0$) and rough soil–wall interface ($\delta = \varphi$) for $\varphi = 30°$. When a smooth soil–wall interface is considered, the shear failure surface is linear and oriented from the wall base to the ground surface and the failure angle (θ) is about 29.214° (Figure 8a). The angle of the failure plane, concerning horizontal direction, is approximately equal to the theoretical value by Rankine theory, i.e., $\theta = \tan^{-1}(45 - \varphi/2) = 29.985°$ [1]. In contrast, Figure 8b shows that the shear failure surface is somewhat curved log-spiral one for a rough soil–wall contact. The corresponding predicted failure mechanism is quite similar to that of the limit equilibrium Prandlt's solution.

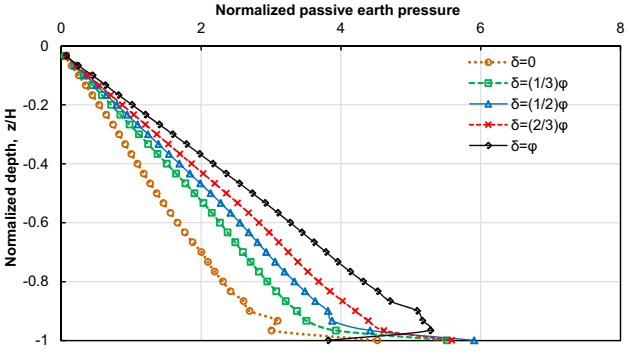

Figure 7: Normalized earth pressure versus normalized depth for rigid wall subjected to translation movement ($\varphi = 30°$).

Using the critical state concept, Fang et al. [10] analyzed the effect of the relative density (D_r) of backfill material on the PEP. The experiments were performed for horizontal cohesionless backfill material retained by a vertical rigid wall undergoing horizontal translation movement. Fang et al. [10] concluded, for a loose backfill material ($D_r = 38\%$), that the passive condition occurred when the normalized wall displacement is about $S_{max}/H = 0.17$. In the case of medium dense ($D_r = 63\%$) and very dense ($D_r = 80\%$) backfill material, the peak of PEPs were recorded for normalized horizontal displacements of $S_{max}/H = 0.03$ and $S_{max}/H = 0.01$, respectively. After that, adopting the residual shear strength of backfill material, the predicted PEP is reduced; the ultimate passive force was recorded at normalized horizontal displacement $S_{max}/H = 0.10$ for medium dense backfill material and $S_{max}/H = 0.20$ for dense backfill material. Table 1 compares PEP's predicted coefficient (K_p) by FLAC code with those suggested by Fang et al. [10].

The present analysis results provide an acceptable estimation of the PEP coefficient (K_p) with a maximum relative difference of –20.84, 9.54, and 6.82% for the dense, medium dense, and loose backfill materials, respectively. When adopting the peak shear strength for the dense backfill material, the maximum difference in the normalized horizontal displacement is equal to 50%. Indeed, in the case of dense sand, from Table 1, the normalized horizontal displacement is between 0.01 and 0.2. Based on the maximum relative differences of K_p values, one notes that friction angles adopted by Fang et al. of 42.1°, 38.30°, and 33° for dense, medium, dense, and loose sands, respectively, are overestimated. More likely, Fang et al. [10] adopted those failure values in a range exceeding the small strain one, i.e., greater than 5%.

Indeed, for sands, current friction angle values of those three density states are rather equal to 28–29°, 30–31°, and 38–39°, respectively Kérisel and Absi [11]. As such, the high relative difference for the dense sand can be argued.

4 Analysis of rigid wall under rotational movement

Early experimental work presented by Fang et al. [4] showed a nonlinear distribution for the PEP on the rigid

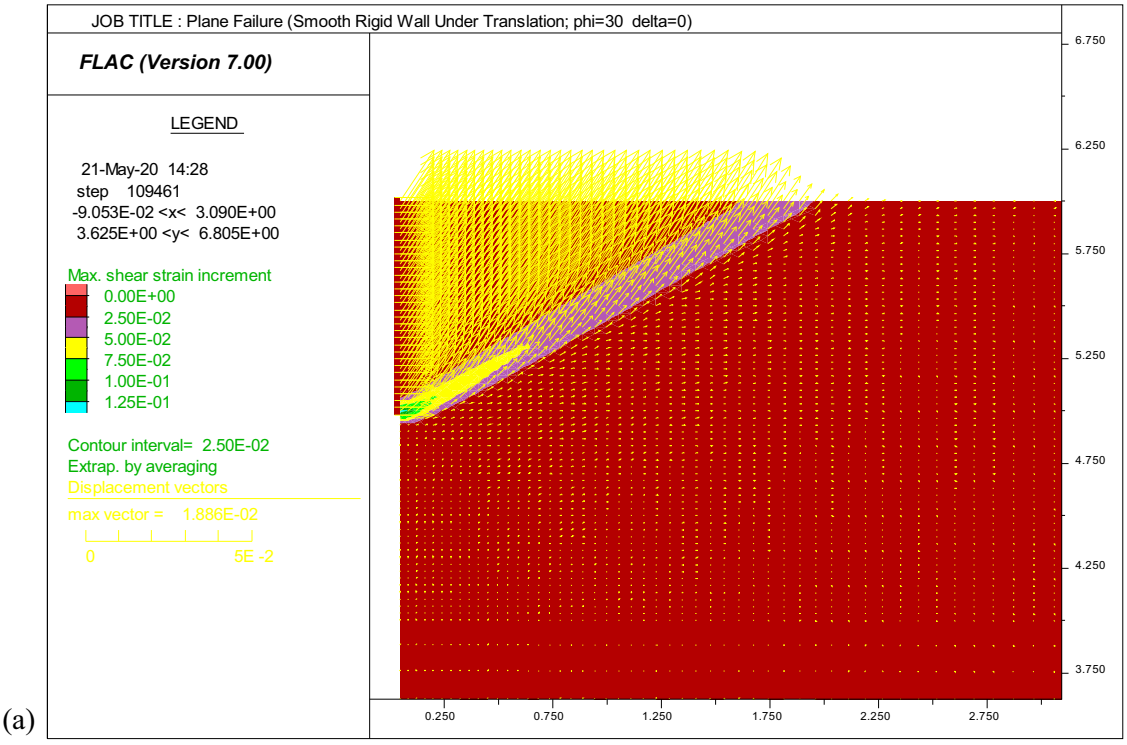

(a)

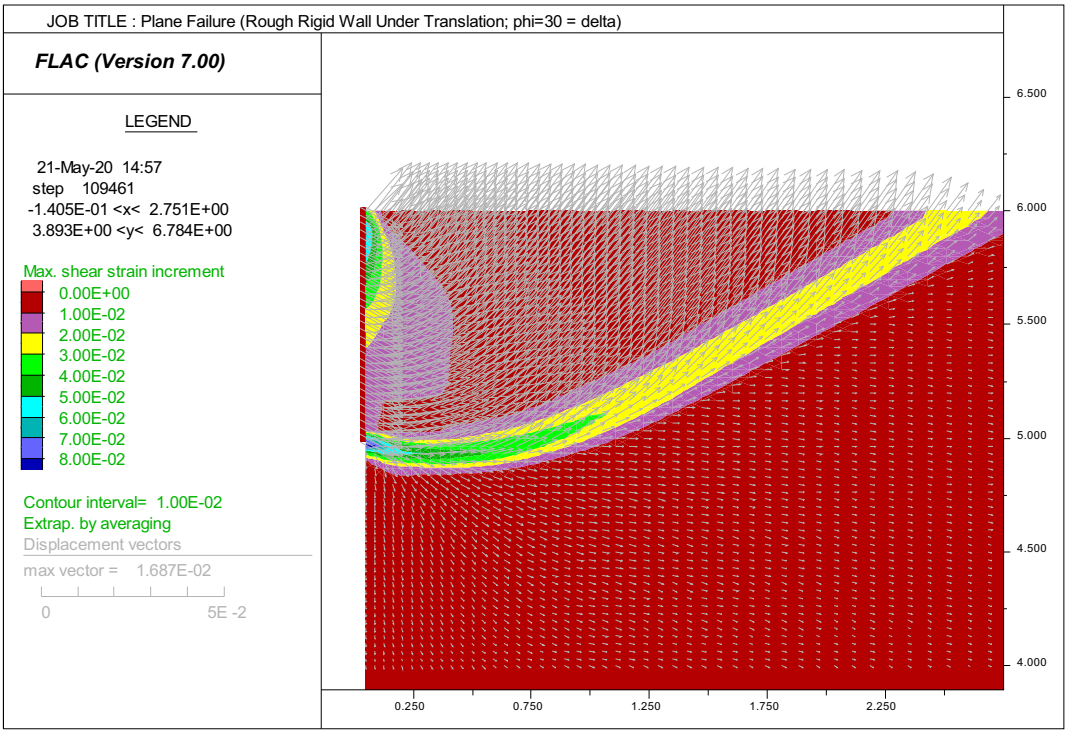

(b)

Figure 8: Distribution of shear strains behind a rigid wall subjected to the horizontal movement for smooth and rough contacts with the backfill material ($\varphi = 30°$). (a) Smooth soil–wall interface ($\delta = 0$), (b) rough soil–wall interface ($\delta = \varphi$).

wall, which depends on the wall movement's type before reaching the failure phase. Experimental results of those authors are used to assess the predictions by the present numerical analysis. The main parameters used in the study are the backfill material's friction angle $\varphi = 30.9°$ and the friction angle of soil–wall is $\delta = 19.2°$. When a

Table 1: Comparison of predicted K_p and S_{max} values with recorded data by Fang et al. [10]

Shear strength	Backfill density	D_r (%)	δ (°)	φ_p (°)	Fang et al. [6]		Present analysis	
					K_p	S_{max}/H	K_p	S_{max}/H
Peak shear strength	Loose	38	9.8	33.0	5.0	0.17	5.366	0.17
	Medium	63	12.6	38.3	6.5	0.03	6.500	0.03
	Dense	80	14.0	42.1	8.2	0.01	6.786	0.02
Residual shear strength	Loose	38	9.8	31.5	5.0	0.17	5.008	0.17
	Medium	63	12.6	31.5	4.8	0.10	5.306	0.11
	Dense	80	14.0	31.5	4.8	0.20	5.453	0.20

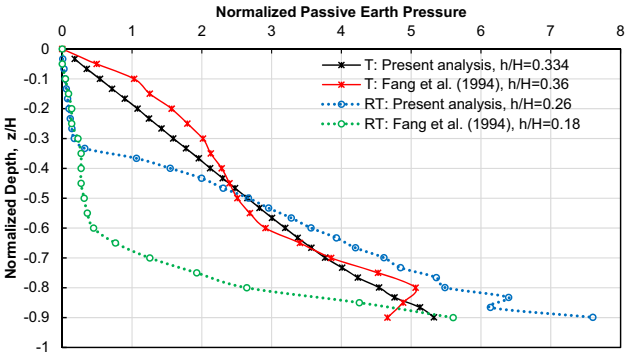

Figure 9: Distribution of PEP with experimental results by Fang et al. [4] (φ = 30.9° and δ = 19.2°).

rigid wall undergoes a translation movement, Figure 9 indicates that the variation of experimental normalized PEP with depth well agrees with the predicted one up to a normalized depth equal to 0.8. Precisely, from the ground surface to a depth equaling to 0.38H, numerical predictions are underestimated compared to the experimental results; the maximum relative difference equals 24%. Meanwhile, for depth between 0.38 and 0.8H, the numerical predictions overestimate the experimental results obtained by Fang et al. [4] with a maximum relative difference of 23%.

From Figure 9, when a rigid wall undergoes a rotation around the top RT, between depths 0.37 and 0.95H, the predicted PEP significantly overestimates the recorded values [4]. The experimental centroid is located at a depth equal to 0.18H above the rigid wall base (Table 2). However, the predicted numerical centroid equals 0.26H above the rigid wall base. The relative difference between the two results is not negligible, i.e., 30.77%. Although the experimental and numerical normalized horizontal displacement of the rigid wall is in good agreement, the discrepancy in terms of recorded and predicted passive stresses can be attributed to the adopted value of soil–wall contact's friction angle.

From the results suggested by Fang et al. [4], one concludes that the magnitude of the passive force and its location significantly depend on the type of wall movement (Figure 9).

Further, the assessment of numerical predictions using Dou et al.'s [5] experimental data leads to a good agreement between the values of the centroid of passive force predicted by FLAC 2D code which clearly appears in Table 3. For the loose and the medium dense backfill, the maximum relative difference is 0.57 and 0.09%, respectively. However, for the dense sand case, the passive force's centroid is applied at depth of 0.8032H, which is slightly different from the experimental result, i.e., 0.735H. Scatter is about 8.18% for recorded data and 7.28% for analytical results. Also, at depths less than 0.3H, there is no effect of the relative density of the backfill material on PEP's value; the numerical results agree well with those recorded from the experiments.

Figure 10 shows that the predicted PEP in loose sand is not confirmed by Dou et al. [5] results, significantly beyond a normalized depth equal to 0.5. In turn, for medium and dense sands, FLAC predictions are in good

Table 2: Predicted maximum horizontal displacement, S_{max}, and the centroid of PEP force compared with results of Fang et al. [4]

Wall movement	φ (°)	δ (°)	Fang et al. [4]		Present analysis	
			S_{max}/H	Centroid	S_{max}/H	Centroid
Translation (T)	30.9	19.2	0.18	0.36	0.18	0.334
Rotation around the top (RT)			0.20	0.18	0.20	0.260

Table 3: Comparison of the calculated centroid of PEP with results of Dou et al. [5]

Backfill density	φ (°)	δ (°)	The centroid of earth pressure from the soil surface		
			Dou et al. [5]		Present analysis
			Experimental	Theoretical	
Loose sand	32.60	10.87	0.7547	0.7796	0.7590
Medium sand	34.00	11.33	0.7786	0.7827	0.7793
Dense sand	42.99	14.33	0.7375	0.7448	0.8032

agreement with recorded data. Figure 10 shows the validation of FLAC 2D code predictions by the experimental results up to a depth equals the half of the wall height for medium sand retained by a rigid wall rotating around its top.

Beyond this depth, the results obtained by FLAC 2D code overestimate the experimental results by 33%. The results shown in Figure 10 show that the predicted PEP by the FLAC 2D code for loose, medium, and dense backfill materials underestimates the experimental results up to a depth equal to $0.63H$. Beyond this depth, this trend is reversed.

5 Recommended design parameters

The proposed numerical model was used to investigate the effects of the friction angle (φ) of backfill material and the contact friction angle (δ) between the soil and rigid wall on the PEP coefficient and the centroid of resultant of passive pressure. Table 4 summarizes the calculated PEP coefficient and centroid for five values of the friction angle of backfill material (φ = 20°, 25°, 30°, 35°, and 40°)

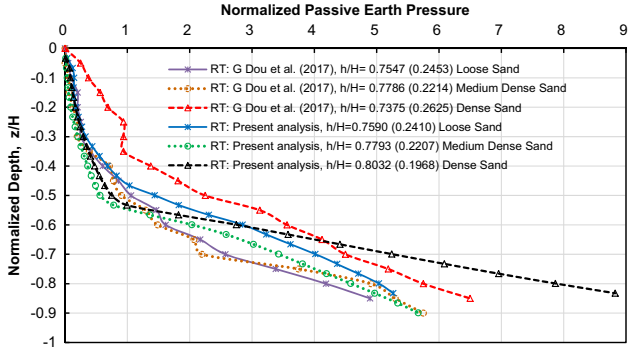

Figure 10: Variation of the PEP with depth from experimental results [5] and predictions by the numerical analysis.

and five values of contact friction angle (δ = 0, 0.333φ, 0.5φ, 0.667φ, and φ). Overall, the predicted PEP coefficient and centroid in the present work, for both T and RT movements, are in good agreement with earlier solution suggested by Kérisel and Absi [11]. Moreover, the predicted PEP coefficient for translation movement (T) is higher than that of rotational movement (RT).

Figure 11 shows, in normalized scale, in case of RT movement, the variation of the PEP with depth for different values of the contact friction angle (δ) between the soil and wall and the friction angle of backfill material is (φ = 30°). It is evident from the results shown in Figure 11 that the normalized PEP is marginal and not influenced by the contact friction angle (δ) from the top of the wall to a depth equal to $0.4H$. Then, from depth equaling to $0.4H$ to a depth equaling to $0.83H$, the normalized pressure increases linearly with a noticeable effect on the contact angle (δ). In this range of depth, when the value of δ increases, the PEP also increases. There is an arbitrary distribution at depth greater than $0.94H$ for the normalized PEP, which can be related to the boundary conditions at the base of the rigid wall both for the T and RT movements.

Based on the results shown in Figure 12, it is clear at depth equaling to $0.32H$ from the wall base in the case of translation movement, the centroid of PEP is almost constant. Therefore, the soil–wall friction angle (δ) and the friction angle of backfill material (φ) have negligible effects on the variation of PEP with depth. The centroid of passive earth distribution decreases significantly in the range from 0.259 to $0.164H$ measured from the rigid wall base in the case of rotational movement (RT). In this case, one concludes the noticeable effects both of angles (δ) and (φ) on the predictions

A slight change was noticed in PEP's magnitude when the contact friction angle (δ) increases from zero to φ. The centroid of PEP moves towards the wall base due to the increase in the soil density and its friction angle. Therefore, the horizontal displacement of the wall can be neglected. The present analysis's numerical predictions

Table 4: Comparison of K_p and the centroid of the resultant of PEP as obtained from the present analysis with Kérisel and Absi [11] solution

φ (°)	φ/δ	Kérisel and Absi [11]		Present analysis			
				T-mode		RT-mode	
		K_p	Centroid	K_p	Centroid	K_p	Centroid
20	0	2.05	0.333	2.076	0.322	2.052	0.235
	1/3	2.40		2.403	0.327	2.311	0.240
	1/2	2.55		2.564	0.328	2.438	0.246
	2/3	2.75		2.720	0.329	2.549	0.249
	1	3.10		2.956	0.336	2.717	0.259
25	0	2.45	0.333	2.515	0.320	2.45	0.214
	1/3	3.10		3.079	0.326	2.893	0.223
	1/2	3.40		3.376	0.327	3.110	0.232
	2/3	3.70		3.676	0.329	3.283	0.239
	1	4.40		4.205	0.336	3.658	0.241
30	0	3.00	0.333	3.070	0.316	2.970	0.196
	1/3	4.00		4.024	0.325	3.685	0.210
	1/2	4.60		4.571	0.326	4.040	0.220
	2/3	5.30		5.163	0.330	4.313	0.234
	1	6.50		6.291	0.340	5.070	0.236
35	0	3.70	0.333	3.786	0.311	3.651	0.183
	1/3	5.40		5.418	0.325	4.828	0.203
	1/2	6.50		6.480	0.326	5.479	0.213
	2/3	8.00		7.669	0.327	6.170	0.217
	1	10.50		10.180	0.332	7.703	0.218
40	0	4.50	0.333	4.729	0.309	4.381	0.164
	1/3	7.60		7.605	0.323	6.397	0.183
	1/2	9.60		9.676	0.323	7.817	0.192
	2/3	12.00		11.970	0.328	9.511	0.202
	1	18.00		18.710	0.351	13.560	0.225

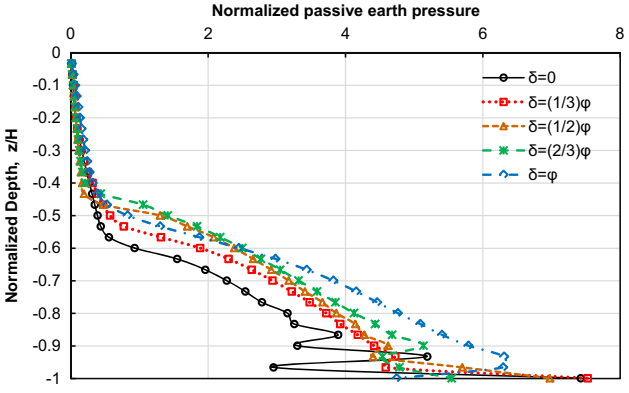

Figure 11: The effect of contact angle (δ) on the variation of the normalized PEP (φ = 30° and RT-movement).

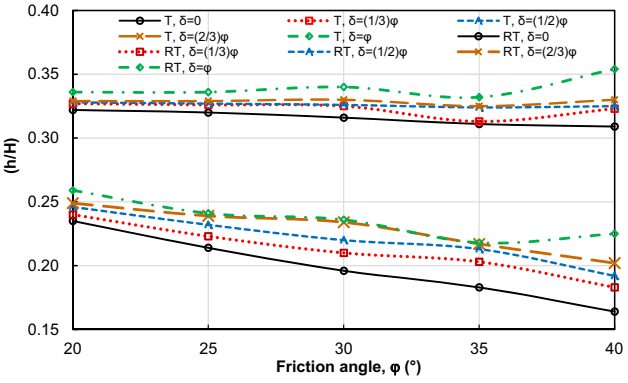

Figure 12: Location of the resultant of PEP for various friction angles of the backfill material considering translation and rotation around the wall movements.

indicate that PEP's centroid can be taken to H/3 from the wall base for a horizontal translation movement (T). However, the centroid of PEP for rotation about the top of the wall (RT) is lesser than H/3 from the wall base. Values given in Table 5 are recommended for estimating the centroid of PEP on a rigid wall undergoing a rotational movement about its top.

6 Conclusion

This paper aims at the numerical determination of the passive earth force generated by a rigid wall movement, either in translation or in rotation around the top, against a purely frictional soil. Implemented parametric study

Table 5: The recommended centroid of PEP for several backfill materials

Angle of friction of backfill material φ (°)	20	25	30	35	40
Distance from the base of wall to the resultant of PEP	0.235–0.259H	0.214–0.241H	0.196–0.236H	0.183–0.218H	0.164–0.225H

considered the influence of the friction angle, e.g., density, of the cohesionless soil and the soil–wall friction angle on the PEP.

The main findings from the numerical analysis conducted by the 2D FLAC code are the following:

- The type of wall movement highly influenced the resultant of the PEP and its location. Good agreements are observed between the obtained numerical predictions, analytical results by Kérisel and Absi (1990), and experimental data proposed by Fang et al. (1994, 2002) and Dou et al. (2017).
- The variation of the PEP force predicted by the proposed numerical wall model for translation and rotation around the top movements (T and RT) is in good accordance with those obtained from previous studies.
- For a horizontal movement of a rigid wall (of height H) and various friction angles of backfill material, the numerical predictions showed a linear variation of the earth pressure with depth. Besides, passive pressure is located between 0.309 and 0.354H from the wall base. However, a nonlinear variation of the PEP was predicted in the case of rotational movement (RT), and the resultant of passive pressure is located at 0.4H from the wall base.
- The distance between the resultant of PEP and the wall base decreases as the backfill material density increases.
- The centroid of PEP is somewhat different from the classical solutions' values when the rigid wall experienced rotational movement around its top. The centroid is approximately under 1/3H estimated from the wall base. Therefore, consideration of the suggested values (given in Table 5) is more useful for the analysis of rigid retaining walls subjected to rotational movement around the top.
- The proposed results require further developments by investigating other types of walls and related movements by using other numerical codes. In such a way, much better update of recommendations for the design of retaining walls can be confirmed.

Acknowledgments: The authors thank the staff of the University of Mohamed Chérif Messaadia, Souk Ahras/Algeria, Staff of Civil Engineering at University of Baghdad/Iraq, and Staff of University of El Manar, Tunis, Tunisia for their help. Also, thanks extended to the General Directorate of Scientific Research and Technological Development (DGRSDT); Ministry of Higher Education and Scientific Research/Algeria for support publishing this work.

Author contributions: Conceptualization: M. F. B., M. O. K., and M. B.; methodology: M. F. B. and M. O. K.; software: M. F. B.; validation: M. F. B.; formal analysis: M. F. B. and M. B.; investigation: M. F. B.; resources: M. F. B.; writing original draft preparation: M. F. B.; writing – review and editing: M. F. B., M. O. K., and M. B.; visualization: M. O. K. and M. B.; supervision: M. B.; project administration: M. O. K.; funding acquisition: M. F. B. All authors have read and agreed to the published version of the manuscript.

Conflict of interest: The authors declared no conflict of interest.

References

[1] Rankine WJM. On the stability of loose earth. Philos Trans R Soc Lond. 1857;147:9–27.
[2] Coulomb CA. Essai sur une application des règles de maximis et minimis à quelques problèmes de statique relatifs à l'architecture. Paris: Mém Math Phys Acad Roy Sci par divers Savants; 1776. p. 7 (in French).
[3] Roscoe KH. The influence of strains in soil mechanics. Géotechnique. 1970;20(2):129–70. doi: 10.1680/geot.1970.20.2.129.
[4] Fang YS, Chen TJ, Wu BF. Passive earth pressures with various wall movements. J Geotech Eng. 1994;120(8):1307–23. doi: 10.1061/(ASCE)0733-9410(1994)120:8(1307).
[5] Dou G, Xia J, Yu W, Yuan F, Bai W. Non limit passive soil pressure on rigid retaining walls. Int J Min Sci Technol. 2017;27(3):581–7. doi: 10.1016/j.ijmst.2017.03.020.
[6] Gong CI, Wei G, Xu RQ. Earth pressure against rigid retaining wall rotating about top. Yantu Lixue (Rock Soil Mech). 2006;27(9):1588–92.
[7] Matsuzawa H, Hazarika H. Analyses of active earth pressure against rigid retaining wall subjected to different modes of movement. Soils Found. 1996;36(3):51–65. doi: 10.3208/sandf.36.3_51.
[8] Hazarika H, Matsuzawa H. Wall displacement modes dependent active earth pressure analyses using smeared shear band method with two bands. Comput Geotech. 1996;19(3):193–219. doi: 10.1016/0266-352X(96)00003-1.

[9] Potts DM, Fourie AB. A numerical study of the effects of wall deformation on earth pressures. Int J Numer Anal Method Geomech. 1986;10(4):383–405. doi: 10.1002/nag.1610100404.
[10] Fang YS, Ho YC, Chen TJ. Passive earth pressure with critical state concept. J Geotech Geoenviron Eng. 2002;128(8):651–9. doi: 10.1061/(ASCE)1090-0241(2002)128:8(651).
[11] Kérisel J, Absi É. Active and passive earth pressure tables. London: CRC Press, Taylor & Francis Group; 1990.
[12] Chen FQ, Lin YJ, Yang JT. Passive Earth pressure of narrow cohesionless backfill against rigid retaining walls rotating about the base. Int J Geomech. 2021;21(1):06020036.
[13] Muni T, Devi D, Baishya S. Parametric study of sheet pile wall using ABAQUS. Civ Eng J. 2021;7(1):71–82.
[14] Karkush MO, Ahmed MD, Sheikha AAH, Al-Rumaithi A. Thematic maps for the variation of bearing capacity of soil using SPTs and MATLAB. Geosciences. 2020;10(9):329.
[15] Narain J, Saran S, Nandakumaran P. Model study of passive pressure in sand. J Soil Mech Found Div. 1969;95(4):969–84. doi: 10.1061/JSFEAQ.0001318.
[16] Shiau JS, Augarde CE, Lyamin AV, Sloan SW. Finite element limit analysis of passive earth resistance in cohesionless soils. Soils Found. 2008;48(6):843–50. doi: 10.3208/sandf.48.843.
[17] FLAC. Fast Lagrangian Analysis of Continua, version 7.0. Minneapolis: Itasca Consulting Group, Inc.; 2007.
[18] Benmeddour D, Mellas M, Frank R, Mabrouki A. Numerical study of passive and active earth pressures of sands. Comput Geotech. 2012;40:34–44. doi: 10.1016/j.compgeo.2011.10.002.
[19] Salençon J. Introduction to the yield design theory and its applications to soil mechanics. Eur J Mech A Solids. 1990;9(5):477–500.
[20] Soubra AH, Macuh B. Active and passive earth pressure coefficients by a kinematical approach. Proc Inst Civ Eng Geotech Eng. 2002;155(2):119–31. doi: 10.1680/geng.2002.155.2.119.